Characterization of the Virgo Seismic Environment

Michael W. Coughlin[1, a]

[1] *Carleton College, One North College Street, Northfield, Minnesota 55057*

An important consideration for Virgo is to characterize the seismic environment near the detector and understand how environmental effects from the surrounding area couple into the interferometer. During the months of June and July 2010, a Guralp-3TD seismometer was stationed at various locations around the Virgo site. Seismic data were taken and examined, with spectral analysis and coherence with seismometers inside of the detector performed. Environmental effects were noted and attempts were made to identify their sources.

PACS numbers:

I. INTRODUCTION

The general theory of relativity predicts that all accelerating objects with non-symmetric mass distributions produce gravitational waves (GW). GW presumably should be directly detectable when very massive objects such as black holes or neutron stars undergo acceleration. LIGO (the Laser Interferometer Gravitational-Wave Observatory) [1] and Virgo [2] are some of the detectors searching for GW. These experiments seek to directly detect GW and use them to study astrophysical sources. They seek GW associated with the inspiral of binary neutron stars and black holes and the merger of these, GW burst from supernovae and gamma ray sources, periodic GW from nonaxisymmetric rotating or vibrating neutrons stars, and processes of the early universe which would produce a stochastic background of GW. [1].

In 2011, Virgo, located in Cascina, Italy, expects to undergo upgrades, known as "Advanced Virgo," to improve its sensitivity by an order of magnitude [3]. This interferometer has resonant, Fabry-Perot arm cavities with light from lasers traveling down each of the arms [2]. The Virgo detector is sensitive to a variety of noise sources of non-astrophysical origin, such as instrumental glitches, environmental disturbances, and mechanical resonances. Events not caused by GW in the data often produce significant effects in interferometers, as there is significant power in these signals. These instrumental and environmental artifacts make it difficult to identify a GW unambiguously.

Seismic noise places a limit on Virgo's detection sensitivity. Although Virgo's mirrors are well-isolated from local seismic activity by suspension systems made of multi-stage pendulums, seismic noise remains a concern. One path of seismic noise is that of "diffused light" [4]. Because of unavoidable imperfections in the detector's optical components, some tiny fraction of light can exit the main optical path and hit a surface that is connected to the ground, and thus be subject to the local seismic field. When this light reflects off of mirrors, lenses, or photo-detectors on external optical tables used for detector controls, it is often diffused over a wide solid angle and a fraction of it can re-enter the main beam path but with a slightly different phase (as it took a longer path). This phenomena functions as extra noise in the GW channel and limits its sensitivity.

Because seismic events couple in this way into the GW channel, it is necessary to understand and mitigate the noise from the local seismic environment. To assist in this effort, the Virgo observatory is supplemented with hundreds of sensors, including seismometers and accelerometers, that monitor the local environment [5]. These channels are used to detect environmental disturbances that can couple to the GW channel and are strategically placed in sensitive areas of the interferometer to accomplish this. To reduce the influence of anthropogenic noise, during the Advanced Virgo upgrade, machines that are identified as seismically and acoustically affecting the interferometer will be replaced, moved, or isolated [3]. The current proposal is to move all chillers, water pumps, air compressors, and air conditioners from their current locations to some defined distance from the interferometer. By placing these machines on their own foundation, Virgo hopes to drastically reduce their affect on the detector.

As such, documentation of the local seismic environment is necessary, as well as identification of seismic noise sources reaching the detector from the surrounding environment. On top of this, this project seeks to measure the factor of noise reduced between a machine some distance from the interferometer and the noise in the interferometer itself. In order to accomplish this, during the months of June and July 2010, a Guralp-3TD seismometer was stationed at various locations around the Virgo site. Seismic data were taken and examined, with spectral analysis and coherence

[a] Electronic address: coughlim@carleton.edu

Section Letter	Building Name	Location in Building	Location Compared To	Distance Between Seismometers (meters)
A	Technical Building One	Ground Floor	Central Building: Ground Floor	80
B	Building One	First Floor	Central Building: Ground Floor	105
C	Outside Building One	Ground Floor	Mode Cleaner: Ground Floor	30
D	Outside Mode Cleaner Building	Ground Floor	Mode Cleaner: Ground Floor	10
E/F	West/North End Building	Ground Floor	West/North End Building: External Optical Bench	20

TABLE I: Locations of seismometer placement.

with seismometers inside of the detector performed. Environmental effects were noted and attempts were made to identify their sources. Section 2 discusses the methods used when taking and analyzing data. Section 3 presents the lines found in this analysis at the various locations, while Section 4 provides an estimate for the attenuation of these lines as a function of distance. Appendix A includes maps of the locations studied, while Appendix B provides tables containing information about lines found. Finally, Appendix C provides power spectral density and coherence plots for all of the locations studied.

II. CHARACTERIZATION METHODS

A. Measurement Setup

Using a Guralp-3TD tri-axial velocimeter, specifications for which can be found here [6], data were taken at six locations around the site using a sampling rate of 250Hz. Maps for the site and the locations of the measurements can be seen in Figure 1. These locations were chosen for their proximity to machinery known to create large seismic noise. These locations are detailed in Table I, with the machines at each location in Table II and maps included in Appendix A. For each location, the Power Spectral Density (PSD) of the Guralp seismometer, called also the "test probe," is computed, an example for which can be seen in Figure 2. Each measurement lasts approximately 24 hours in order to determine the hourly and daily cycle operation for the machines. This measurement is compared with a tri-axial seismometer, called also the "reference probe," permanently stationed in the closest nearby experimental area containing sensitive interferometer components [5]. In the Mode Cleaner, West End, and North End Buildings, the reference probe was a Episensor FBA ES-T, while in the Central Building, the probe was a Guralp CNG-T40. To identify the characteristic frequencies for some machines, a PCB accelerometer, specifications for which can be found here [7], was used in conjunction with a spectrum analyzer.

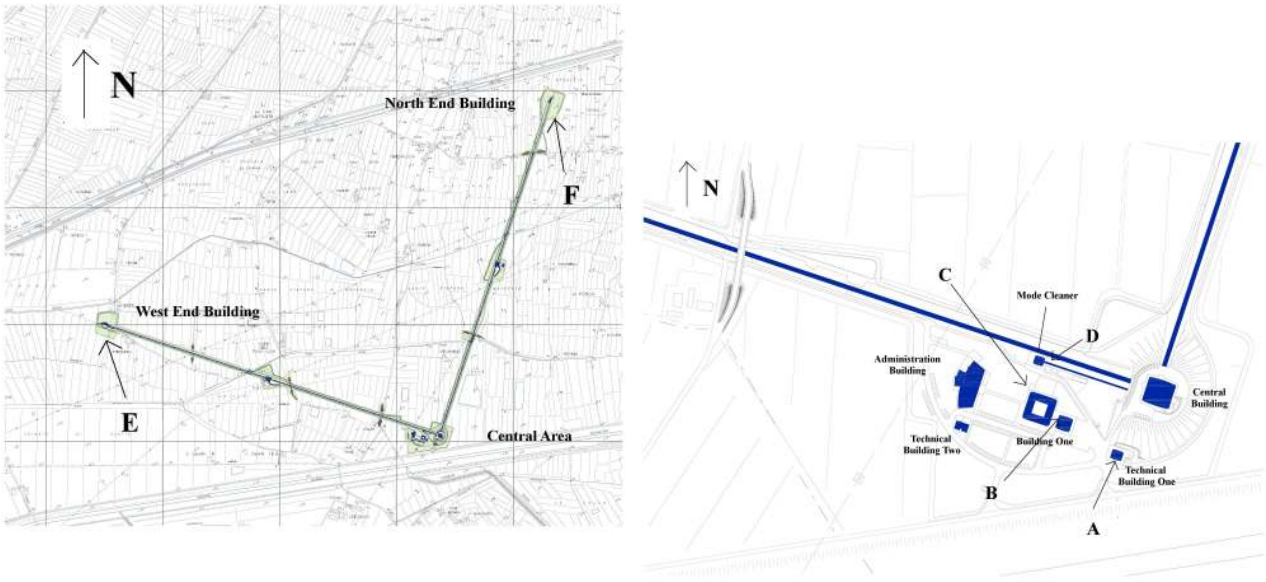

FIG. 1: Left: Arial View of the Virgo Interferometer. Right: Arial view of Virgo's Central Area. Measurement sites are marked with the letter (corresponding to those given in Table I).

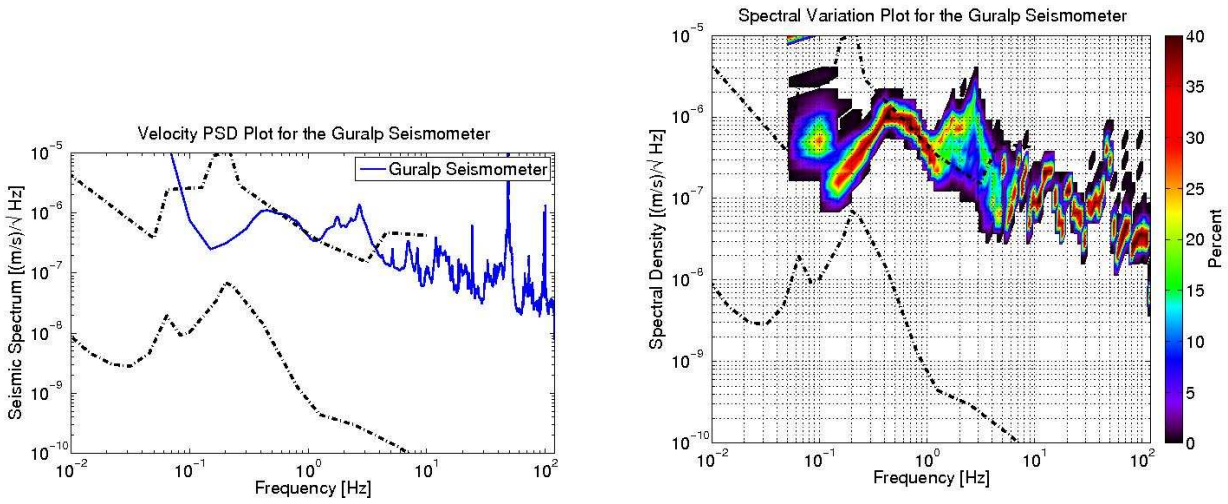

FIG. 2: Left: Averaged root spectral density of the modulus of the the components of the Guralp seismometer at the Virgo site during a day in June of 2010. The two dashed curves correspond to the Peterson low- and high-noise models [8]. Right: Variation in the root spectral density of the seismometer on that same day.

B. Analysis Methods

Important noise components are frequency lines that appear as significantly coherent between the test and reference probes, which establishes the cause of the line being the same in both seismometers. It is also important when these lines are stronger near the machinery than the experimental area, as this indicates the source to be in the machinery and not a source from the experimental area (such as the DAQ or a known resonance). In order to determine when the latter is the case, the PSDs of both seismometers is plotted and examined, which, along with the coherence, can be seen in Appendix C of the paper. Water pumps and cooling fans are some examples of machines giving off continuous lines. If the source is not obvious, suspected machines are analyzed with the PCB accelerometer and spectrum analyzer, comparing the machines' characteristic frequencies to those seen in the coherence. These lines are detailed in tables in Appendix B of the paper.

Periodic lines, on the other hand, are more difficult to identify. Because the lines come and go, they tend to be washed out in PSD averaging. For this reason, Time-Frequency plots of the PSDs are produced and examined by eye for periodic lines. In order to identify the source of these lines, the periodic line must be first quantified in some way. To study the average amplitude of the seismic signal in a frequency band, one can compute the root-mean-square (RMS) in that band, which is defined as:

$$RMS = \sqrt{\sum_{i=1}^{n} {x_i}^2 * \delta f} \tag{2.1}$$

where x_i is the ith component of the frequency band in question and δf is the width of the frequency bins in the spectrum. The sum goes from i=f_1 to i=f_2, where f_1 and f_2 are the minimum and maximum frequencies respectively in the frequency band. This RMS value can then be compared to the time series of various Infrastructure Machine Monitoring System (IMMS) signals, including temperature and pressure probes, to identify their source. All periodic lines found are studied as their effect on the interferometer is more difficult to quantify (due to averaging, proximity to continuous lines, etc.). In the following section, results of these methods are presented for each data record.

In an attempt to quantify the noise mitigated by the distance of the machinery from experimental areas, the ratio of the PSDs of both probes for the identified lines was measured. In this way, a rough estimate of the attenuation factor as a function of distance was measured and presented in Section 4.

III. CHARACTERIZATION RESULTS

A. Characterization of Noise from Technical Building One

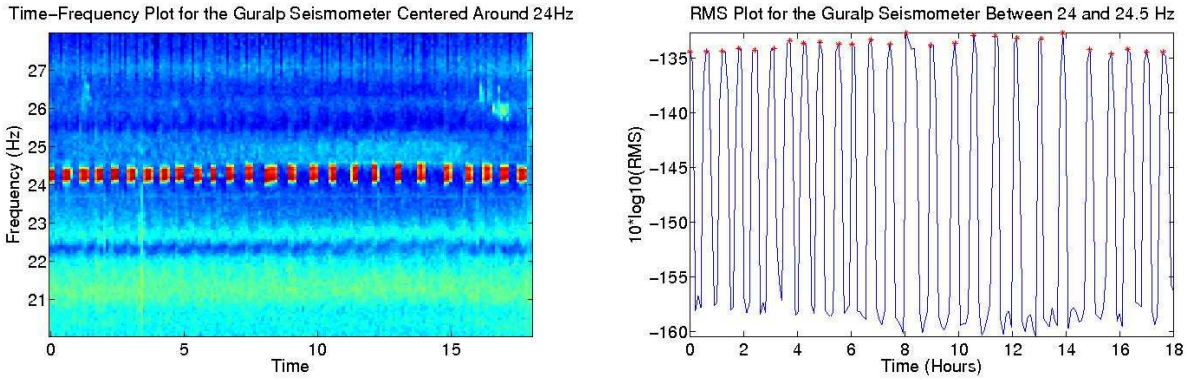

FIG. 3: Left: PSD as a function of time and frequency of the Guralp seismometer in TB1 zoomed in on the 24 Hz region. Right: A plot of the RMS around the periodic line at 24.2Hz of the Guralp seismometer. The red stars correspond to peaks found in the RMS, which provided an estimate of the period and frequency of the line.

The first data were taken in Technical Building One (TB1) and compared with data from a seismometer on the floor of the Central Building (CB), where the two arms of the interferometer converge. These two probes are approximately 80 meters apart. The PSDs of the test and reference probes, as well as the coherence between them, can be seen in Figure 21. These noise lines are documented in Table III. A structure around 24Hz is seen, which is showed in detail on the left of Figure 3. The periodic line, which is at 24.2 Hz with harmonics at 48.4 and 72.6 Hz, was studied closely. The frequency band of the RMS in this case is f_1=24Hz and f_2=24.5Hz, a plot for which can be seen on the right of Figure 3. From this plot, the line's period is estimated at 2492 seconds or about 42 minutes, while the frequency is approximately 0.4mHz.

In order to determine the importance of this periodic noise line, it was necessary to find out if this line was appearing in the CB. To do so, the spectrum of the seismometer permanently stationed in the CB was examined, which can be seen on the left of Figure 5. A clear periodic line around 24.2Hz can be seen in the spectrum, similar to that of the seismometer in TB1. In order to find the source of the periodic line, it was necessary to determine in which building the line was louder. The ratio of the PSDs around 24.2 Hz (Seismometer in TB1/Seismometer in CB) was approximately 16, shown in Figure 4, indicating the source of the line to be in TB1. The coherence around this line was about 0.6, indicating a strong correlation between the two seismometers at that frequency.

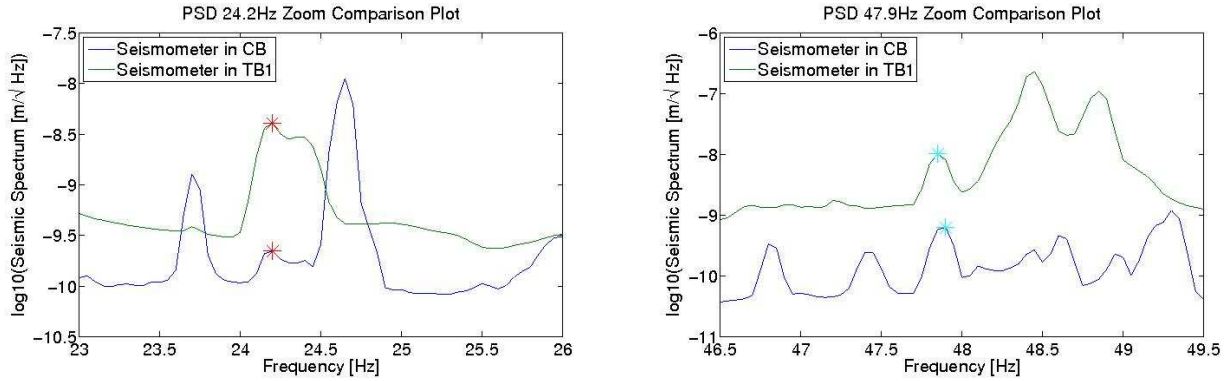

FIG. 4: Left: PSDs of the seismometers in TB1 and the CB around the 24.2Hz periodic line. The peak to the left of the 24.2Hz line is known to be the CB's DAQ room air conditioning unit, while the peak to the right is the scroll pump, which is turned off during science mode. Right: PSDs of the seismometers in TB1 and the CB around the 47.9Hz continuous line.

The time series of a number of monitors of the machinery in TB1 were compared with the RMS of the 24.2Hz signal in the Guralp seismometer, one of which may be seen on the right of Figure 5. From this figure, the RMS in the

24Hz band of the Guralp seismometer is clearly correlated with time series of a temperature monitor of the first water chiller. One can see that when the temperature of the water reaches a high point, the cold water chiller switches on, causing the temperature of the water to decrease. When the temperature reaches a low point, the water chiller switches off and the whole process starts again. The chiller is located on the roof of TB1, as can be seen on the left of Figure 18. It is provided with insulating springs, although it is possible that the vibrations can travel through the rigid water pipes between TB1 and the CB or in the water itself. Better insulation for these parts, such as flex joints, will be studied.

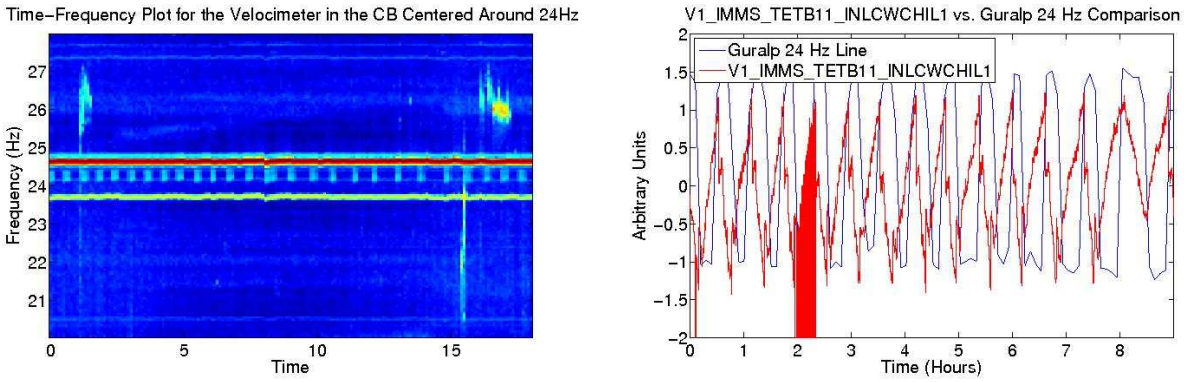

FIG. 5: Left: This plot shows the PSD as a function of time and frequency around 24Hz in the modulus of the three components of the seismometer in the CB. Right: A plot of both the RMS in the 24Hz band of the Guralp seismometer as well as the time series of a temperature monitor of the first (of two) cold water chillers.

B. Characterization of Noise from Building One

The second data were taken in Virgo's Building One (B1) and compared with the same seismometer in the CB. These two probes are approximately 105 meters apart. The PSDs of the test and reference probes, as well as their coherence, can be seen in Figure 22. The noise lines are documented in Table IV. It was suspected that the lines seen in the coherence originated in either the computer fans on the first floor of B1 or the air conditioning units on the roof of B1. In order to check this hypothesis, the characteristic mechanical frequencies of these machinery were examined with the PCB accelerometer, which can be seen in Figure **??**.

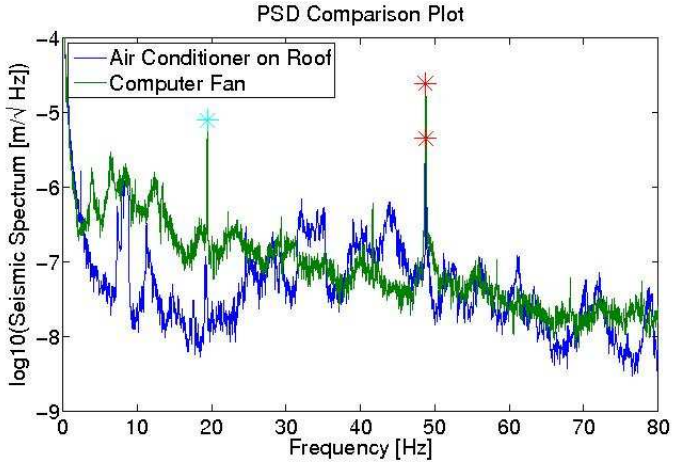

FIG. 6: This plot shows the PSD for both a fan in the computer room as well as an air conditioner on the roof. The data were taken with a portable probe in direct contact with the machines under study. Both show strong lines around 48.4Hz, which are shown by the red stars on the right, and the computer fan shows a strong line around 19.3Hz as well, which is shown by the blue star on the left.

Two of the lines found in the machinery, 19.3Hz and 48.4Hz, matched up well with those frequencies with strong

coherence, and these are suspected to be the source. Shown in Figure 7 are the comparative strengths of these lines in both locations, and both are above the background at both locations, indicating their relevance. The source of the 19.3Hz line is most likely the computer fans, while the 48.4 line could be either of the machines or many others around the site. It is important to note that many Virgo motors are "squirrel double-cage AC Asynchronous Induction Motors," which are common medium-size motors. These motors usually run at half the speed of the frequency of the power main, which in Europe is 50Hz, while smaller motors run at approximately the same speed as the power main. Thus the larger motors run at approximately 25Hz, but due to friction effects, the real rotating frequency is slightly less than this. For this reason, values span around 24Hz for larger (double cage) motors and 48Hz for smaller (single cage) motors. Thus, lines seen near these frequencies can come from multiple sources, including smaller motors and water pumps, and so it is more difficult to exactly identify their exact source. In a previous switch off test of an air conditioning unit in the DAQ room in the CB (described in elog entry 24621), lines around 19.5Hz and 48.8Hz were noted. As machine lines tend to wander, it is possible that the lines seen in the CB are caused by this machine instead.

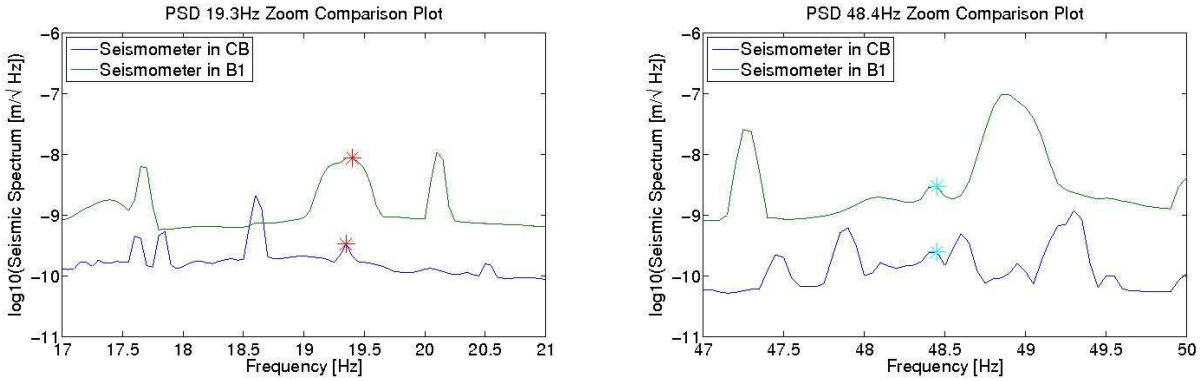

FIG. 7: Left: PSDs of the seismometers in B1 and the CB around the 19.3Hz continuous line. Right: PSDs of the seismometers in TB1 and the CB around the 48.4Hz continuous line.

C. Characterization of Noise from Chillers Outside Building One

The third data were taken on a platform between B1 and the Mode Cleaner Building (MC) and compared with a seismometer in the MC. The MC contains the end mirror of the Input Mode Cleaner optical cavity and filters jitter and power noise as well as higher order modes from the beam. The distance between these probes is approximately 30 meters. On this platform resides two chillers, a small one which serves the Seminar Room (SR) in B1 and a larger one which serves the rest of B1. The PSDs of the test and reference probes, as well as their coherence, can be seen in Figure 23. These noise lines are documented in Table V.

There are no IMMS probes monitoring the processes of these machines, and thus for indentification of periodic lines, information from Virgo personnel is relied on. In order to find the source of the significant noise lines, vibration noise of both chillers was measured using the spectrum analyzer and the portable accelerometer. It is known that the SR chiller is on continuously during the day (from 9 A.M. to 6 P.M.) and turns on during the night when the SR falls below a certain temperature. Similarly, the B1 chiller is only on during the day and not during the night. This effect can be seen in Figure 9, where a line at 60Hz can be seen on continuously during the main working hours (0-6 Hours on the plot) and only periodically during the night, showing that it corresponds to the SR chiller. On the other hand, a broadband line around 90Hz can be seen on during only working hours, thus corresponding to the B1 chiller. Upon comparison with the coherence results, a number of the low frequency lines were identified. Interestingly enough, these high frequency lines are not seen in coherence, while the lower frequency components from the chillers are, two of which can be seen in Figure 8.

D. Characterization of Noise from the Cold Water Chiller Outside the Mode Cleaner

The fourth data were taken outside the MC, on the same concrete platform as the MC's cold water chiller, and compared with the seismometer inside of the MC. The distance between these probes is approximately 10 meters.

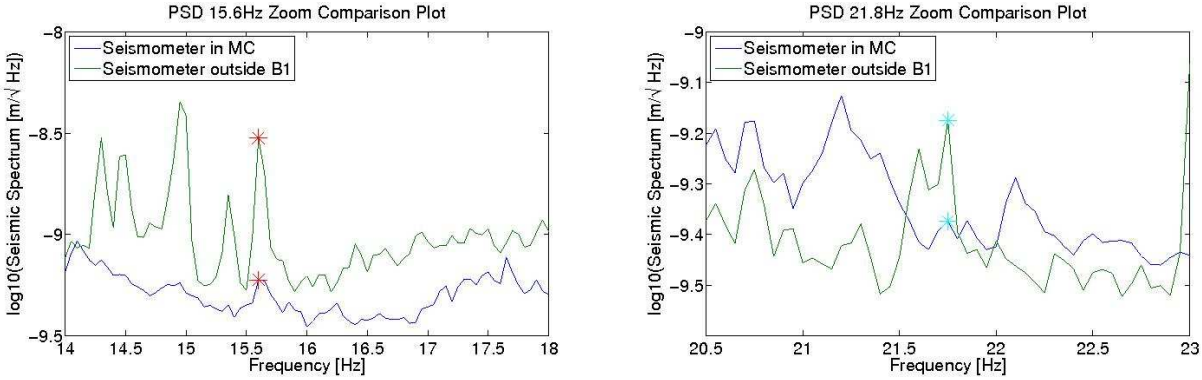

FIG. 8: Left: PSDs of the seismometers outside B1 and in the MC around the 15.6Hz continuous line. Right: PSDs of the seismometers outside B1 and in the MC around the 21.8Hz continuous line.

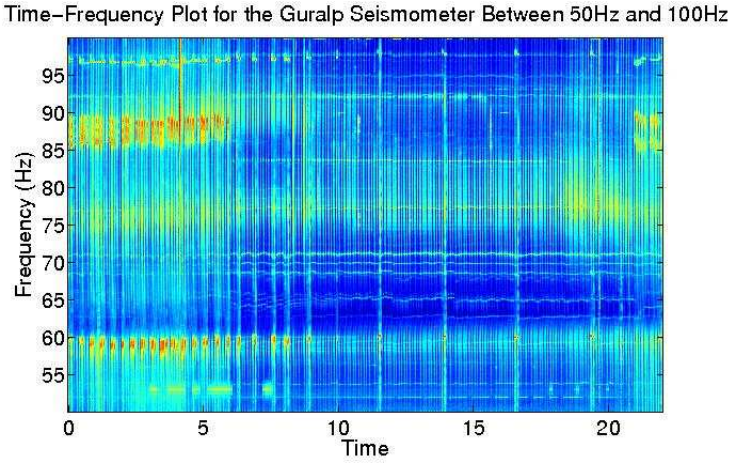

FIG. 9: This plot shows the Time-Frequency plot for the Guralp seismometer placed near the chillers of B1 between 50Hz and 100Hz.

The PSDs of the test and reference probes, as well as the coherence, can be seen in Figure 24. These noise lines are documented in Table VI.

Upon viewing the PSD plots, a number of significant lines are noticed, including continuous lines at 24.2Hz and 38.8Hz, which can be seen on the left of Figure 10. A strong periodic line at 48.9Hz, which has a harmonic at 97.8Hz, can be seen on the right of Figure 10. To study this line, the RMS around the 48.9Hz band was computed and compared to probes inside of the MC. Similar to Section 2, a water temperature probe follows this line well, as can be seen in Figure 11.

E. Characterization of Noise in the West End Building

The fifth data were taken inside the West End Building (WEB) near the machinery and compared with a Episensor seismometer located on the external optical bench. The distance between these probes is approximately 20 meters. The PSDs of the test and reference probes, as well as the coherence, can be seen in Figure 25. These noise lines are documented in Table VII.

Upon viewing the PSD plots, a number of significant lines are noticed, including continuous lines at 24.7Hz, 47.1Hz, and 48.8Hz, which can be seen in Figure 12. Using the PCB accelerometer, the 48.8Hz line was identified as coming from the cold water pump in the WEB. Similarly, the 47.1Hz line was attributed to the warm water pump. Due to the low attenuation of this line between the machinery and experimental area, it is thought that there is a pipe running between the two areas, and this will be investigated further. A number of the lines seen can also be attributed to the air conditioning unit in the WEB. Periodic lines at 22.1Hz and 14.9Hz are also present in the PSD of the test probe. To study these lines, the RMS around both of these bands was computed and compared to probes inside of

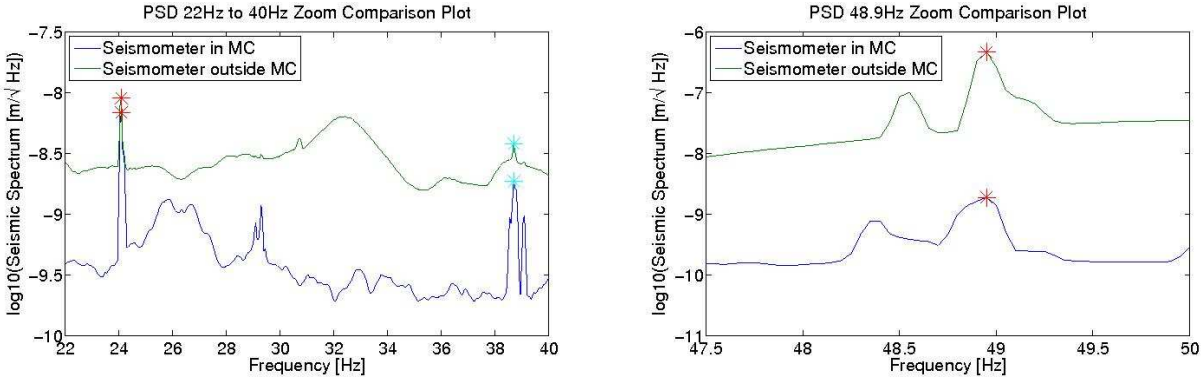

FIG. 10: Left: PSDs of the seismometers outside the MC and in the MC between 22Hz and 40Hz. The red stars on the left correspond to the 24.2Hz continuous line while the blue stars on the right correspond to the 38.8Hz continuous line. Right: PSDs of the seismometers outside the MC and in the MC around the 48.9Hz periodic line.

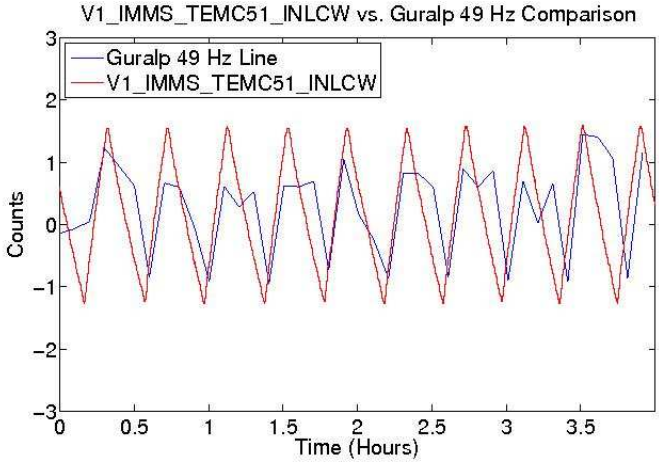

FIG. 11: A plot of both the RMS in the 48.9Hz band of the Guralp seismometer as well as the time series of a temperature monitor of the water chiller.

the WEB. The 22.1Hz line, which has a period of about 49.6 minutes, follows well the temperature probe of a cold water chiller, as can be seen in Figure 13, although it has approximately half the period of the probe. The 14.9 Hz line has a period of approximately 25.7 minutes, but this did not quite follow any of the sensors exactly.

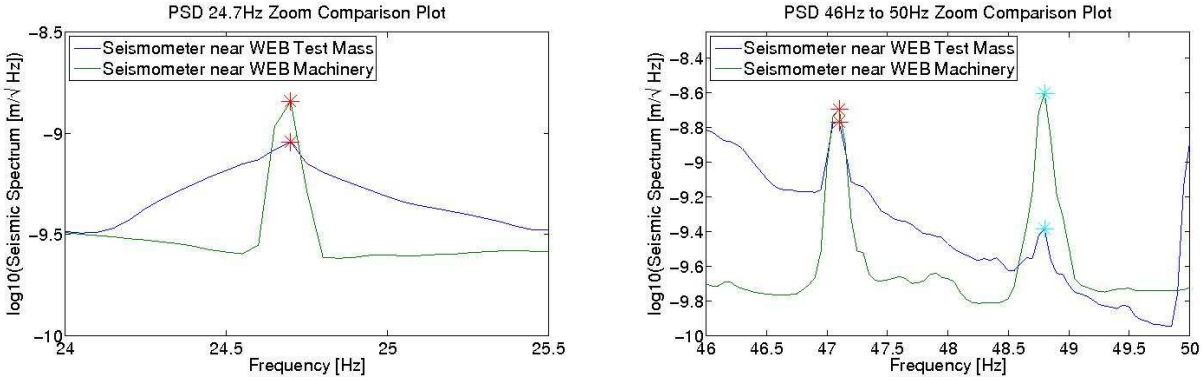

FIG. 12: Left: PSDs of the seismometers near the WEB Machinery and the WEB test mass around the 24.7Hz continuous line. Right: PSDs of the seismometers near the WEB Machinery and the WEB test mass between 46Hz and 50Hz. The red stars on the left correspond to the 47.1Hz continuous line while the blue stars on the right correspond to the 48.8Hz continuous line.

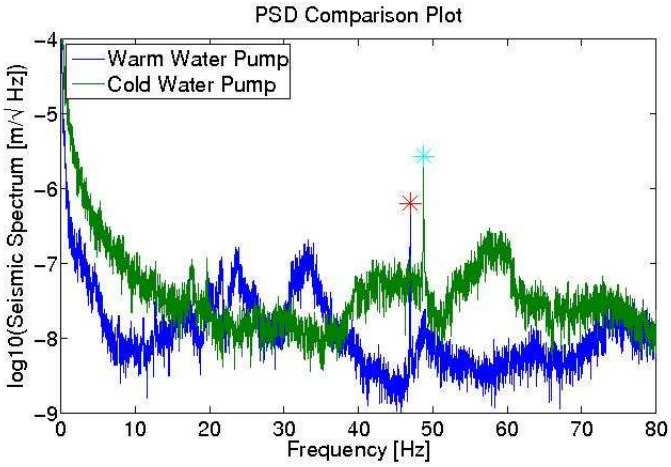

FIG. 13: This plot shows the PSD for both the warm and cold water pumps in the WEB. The data were taken with a portable probe in direct contact with the machines under study. The warm water pumps shows a strong line around 47.1Hz, which is shown by the red star on the right. The cold water pump shows a strong line around 48.8Hz, which is shown by the blue star on the left.

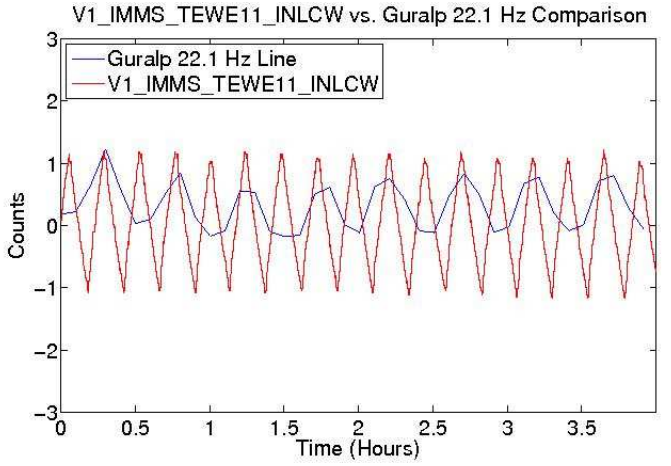

FIG. 14: A plot of both the RMS in the 22.1Hz band of the Guralp seismometer as well as the time series of a temperature monitor of a cold water chiller.

F. Characterization of Noise in the North End Building

The sixth data were taken inside the North End Building (NEB) and compared with a seismometer located on the external optical bench. The distance between these probes is approximately 20 meters. The PSDs of the test and reference probes, as well as the coherence, can be seen in Figure 26. These noise lines are documented in Table VIII.

Upon viewing the PSD plots, a number of significant lines are noticed, including continuous lines at 22.8Hz and 48.7Hz, which has a harmonic at 97.4Hz, which can be seen in Figure 14. A number of the lines can be attributed to the air conditioning unit in the NEB. Similarly, periodic lines at 48.2Hz and 58.8Hz, which has a harmonic at 117.6Hz, are present in the PSD of the test probe. To study these lines, the RMS around both of these bands was computed and compared to probes inside of the NEB. The 48.2Hz line, which has a period of about 108 minutes, follows well the temperature probe of a water heater, as can be seen in Figure 15. The 58.8Hz line has a period of approximately 18.3 minutes, but this did not quite follow any of the sensors exactly.

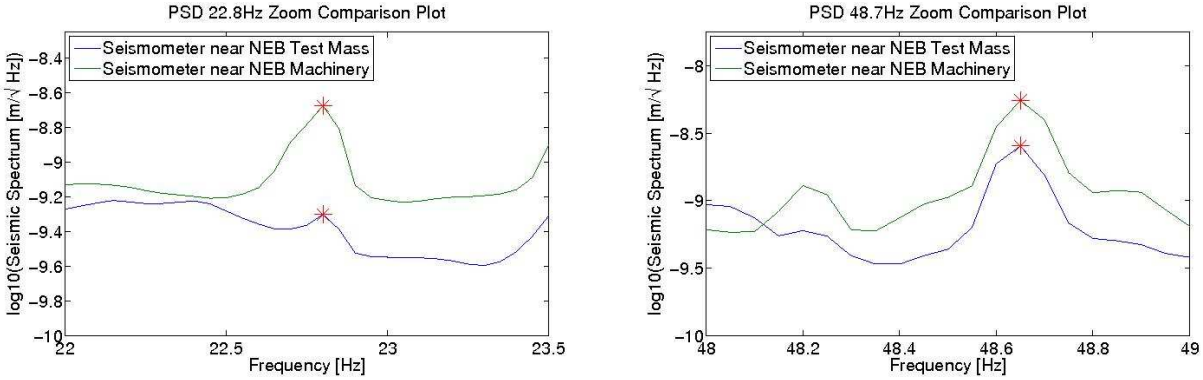

FIG. 15: Left: PSDs of the seismometers near the NEB Machinery and the NEB test mass around the 22.8Hz continuous line. Right: PSDs of the seismometers near the NEB Machinery and the NEB test mass around the 48.7Hz continuous line.

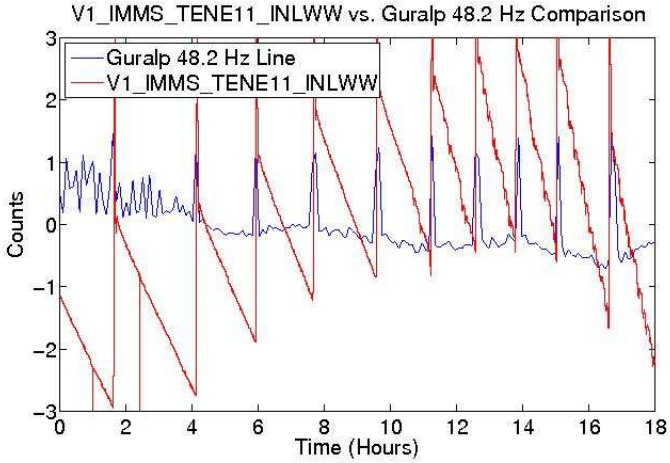

FIG. 16: A plot of both the RMS in the 48.2Hz band of the Guralp seismometer as well as the time series of a temperature monitor of a warm water chiller.

IV. ATTENUATION MEASUREMENT

One of the goals of this project was to attempt to measure how much noise reduction occurs when a machine is own its own foundation and a certain distance away from an experimental area. To measure this attenuation, the PSD ratio of the lines at the different locations were plotted as a function of distance between the probes, the result for which can be seen in Figure 16. A common model for the dissipation of seismic waves from a point source over a distance is $1/sqrt(r)$, where r is the distance from the point source. As can be seen in the plot, distances of less than 40 meters have an attenuation of approximately a factor of 3, and do not follow this model well. This may be because the approximations of the examined machines as point sources over these shorter distances is not a good one. This factor of 3 is smaller than might otherwise be expected and may be due to the resonance of the material between the two different platforms. On the other hand, distances of about 80 meters and greater have values greater than 10 and follow the model well. This is most likely because the machines can more reasonably be approximated as point sources from these distances. From what is known about dissipation of seismic noise through the soil, it is likely that many of the noise sources from the machines a significant distance from the experimental areas are propagating by pipes and other convenient methods between the locations, as they are louder than otherwise might make sense. For this reason, not only seismic isolation for the machines themselves is recommended, but also identification and isolation of these sources is necessary.

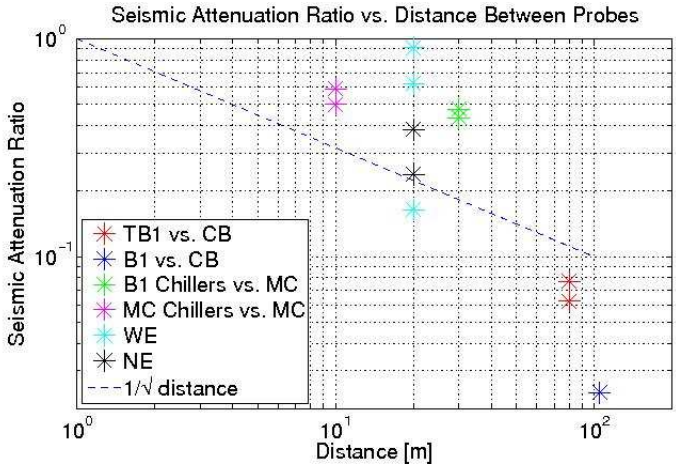

FIG. 17: A plot of the average of the PSD ratio of the coherent lines found in each location as a function of distance between the probes.

V. CONCLUSION

Having found the source of a number of lines, it is difficult to mitigate their affects in the near future. On the other hand, for Advanced Virgo, knowing that the noise from much of the machinery in their current locations reaches the interferometer means that their noise should be mitigated in some fashion. One possibility is to move many of the large instruments to a further distance. From the study in Section 3, as the noise reduction factor is rather small for short distances, the machines identified as significant noise sources should ultimately be seismically insulated using springs, flex joints, and other techniques.

Further beneficial studies might include setting up a noise source with known power and characteristic frequencies on its own foundation at various distances from a sensitive experimental area. This would allow for a comprehensize study of the amount of noise reduced as a function of distance, something this study was limited in.

Acknowledgments

This project is funded by the NSF through the University of Florida's IREU program. The authors gratefully acknowledge the support of the United States National Science Foundation for the construction and operation of the LIGO Laboratory, the Science and Technology Facilities Council of the United Kingdom, the Max-Planck-Society, and the State of Niedersachsen/Germany for support of the construction and operation of the GEO600 detector, and the Italian Istituto Nazionale di Fisica Nucleare and the French Centre National de la Recherche Scientifique for the construction and operation of the Virgo detector. The authors also gratefully acknowledge the support of the research by these agencies and by the Australian Research Council, the Council of Scientific and Industrial Research of India, the Istituto Nazionale di Fisica Nucleare of Italy, the Spanish Ministerio de Educación y Ciencia, the Conselleria d'Economia Hisenda i Innovació of the Govern de les Illes Balears, the Foundation for Fundamental Research on Matter supported by the Netherlands Organisation for Scientific Research, the Polish Ministry of Science and Higher Education, the FOCUS Programme of Foundation for Polish Science, the Royal Society, the Scottish Funding Council, the Scottish Universities Physics Alliance, The National Aeronautics and Space Administration, the Carnegie Trust, the Leverhulme Trust, the David and Lucile Packard Foundation, the Research Corporation, and the Alfred P. Sloan Foundation.

[1] B. Abbott et al. LIGO: The Laser Interferometer Gravitational-Wave Observatory. *Reports on Progress in Physics*, 72, 2009.
[2] F. Acernese et al. Status of Virgo. *Classical and Quantum Gravity*, 25, 2008.
[3] F. Acernese et al. Advanced Virgo Preliminary Design. *Virgo Internal report: VIR-0089A-08*, 2008.
[4] T. Accadia et al. Noise from scattered light in virgos second science run data. *Submitted to GWDAW14 proceedings*, 2010.

[5] F. Barone, F. Garufi, and L. Milano. Environment monitoring parameters. *VIRGO Document VIR-MAN-NAP-5800-102*, 2001.
[6] V. Boschi and A. Gennai. Gralp cmg-3td and cmg-eam quick guide. *VIRGO Document VIR-0172A-10*, 2010.
[7] Piezotronics. Accelerometer model 393b12 specification sheet. *Piezotronics Document*, 2010.
[8] Jon Peterson. Observations and modelling of background seismic noise. *Open-file report*, 1993.

APPENDIX A: BUILDING MAPS

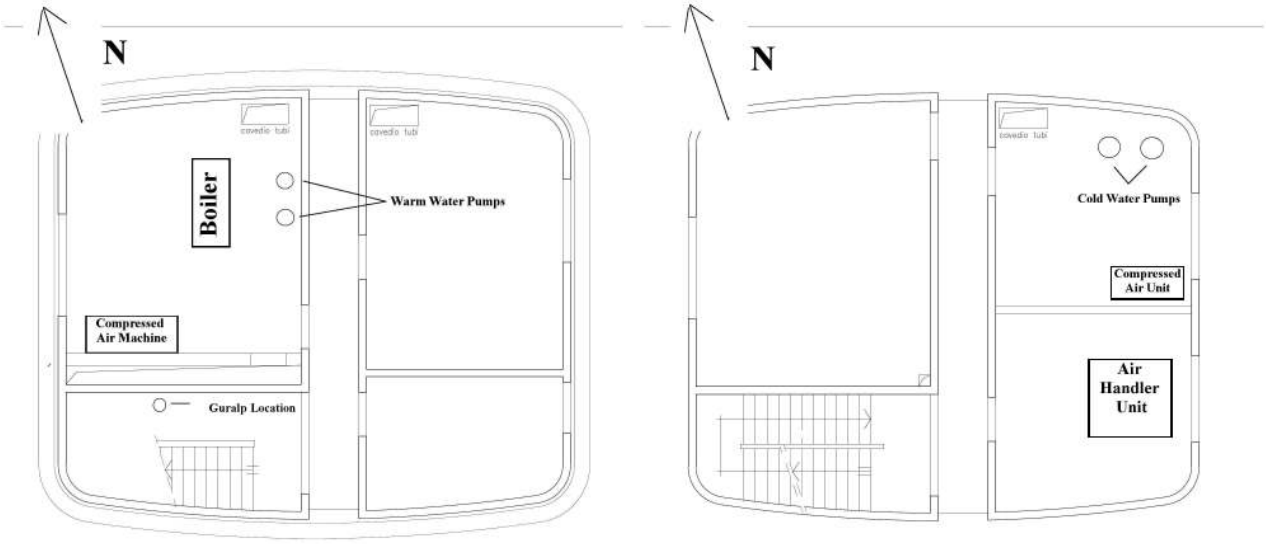

FIG. 18: Left: Map of the ground floor of Technical Building One. Right: Map of the first floor of Technical Building One.

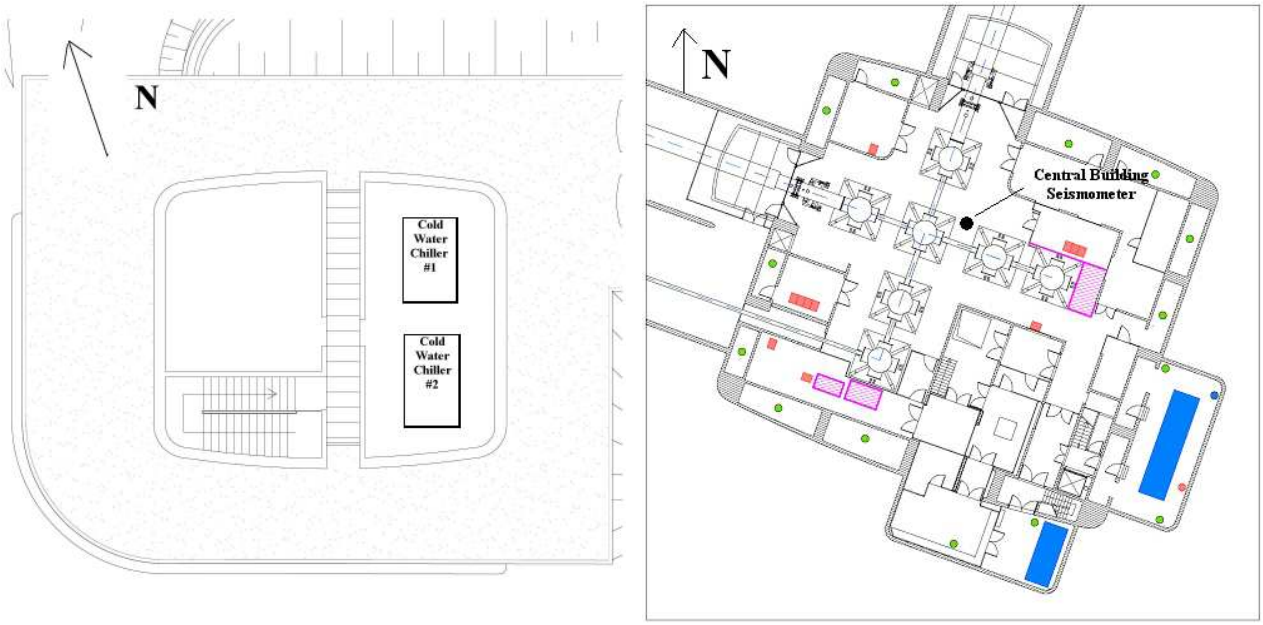

FIG. 19: Left: Map of the roof of Technical Building One. Right: Map of the ground floor of the Central Building.

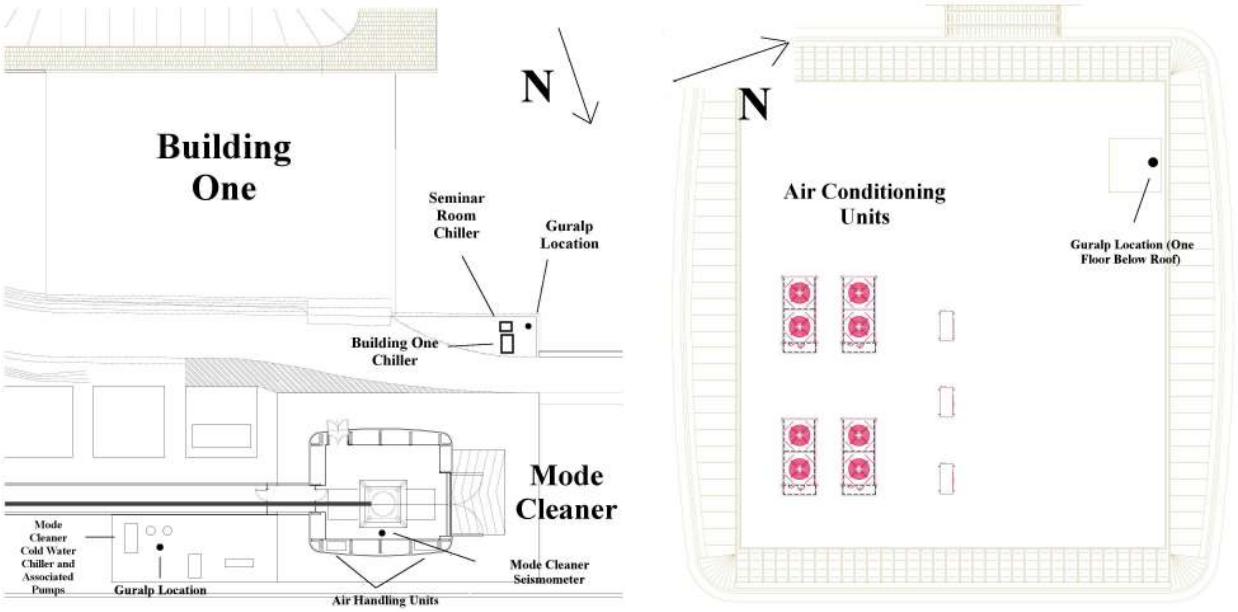

FIG. 20: Left: Map of both Building One and the Mode Cleaner. Right: Map of the roof of Building One.

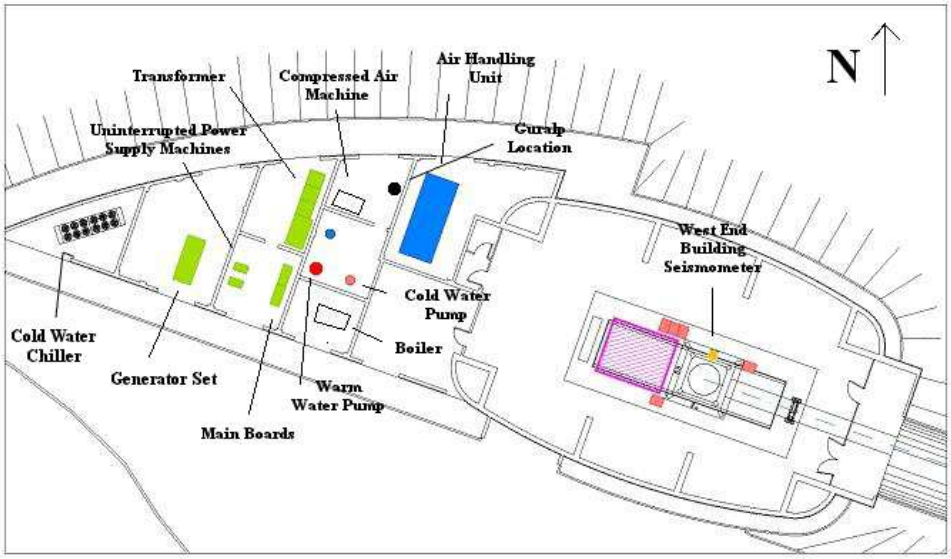

FIG. 21: Map of the West End Building.

Building Name	Known Machinery near Seismometer
Technical Building One	Water Boiler and Pumps, Air Compressor (Ground Floor); Air Handler Unit, Cold Water Pumps, Air Compressor (First Floor); Cold Water Chiller (1 and 2)
Building One	Computer Air Conditioners (First Floor); Building One Air Conditioners (Roof)
Outside Building One	Two Air Conditioners
Outside Mode Cleaner Building	Cold Water Chiller and Pumps
West/North End Building	Cold Water Chiller, Water Boiler, Generator Set, UPS machines, Main Boards, Transformer, Air Compressor, Water Pumps, Air Handler Unit

TABLE II: Information about machinery in measurement locations.

Frequency (Hz)	Periodicity (Period)	Suspected Source	Coherence	PSD in TB1	PSD in CB	PSD Ratio (Test/Reference)
24.2, 48.4,78.6	Periodic (42 Minutes)	Cold Water Chiller 1	0.60	$2.73 * 10^{-9}$	$1.70 * 10^{-10}$	16
47.9	Continuous	Water Pump	0.26	$8.12 * 10^{-9}$	$6.27 * 10^{-10}$	13
65	Periodic (19 Minutes)	Unknown	Negligible	$9.05 * 10^{-11}$	$5.01 * 10^{-11}$	2
67	Periodic (33 Minutes)	Unknown	Negligible	$1.58 * 10^{-10}$	$6.09 * 10^{-11}$	3

TABLE III: Noise lines found in PSD of seismometer in TB1. The table provides the line's frequency, periodicity, suspected source, coherence with a seismometer stationed in the CB, the average PSD of the line in TB1, the average PSD of the line in the CB, and the ratio of those PSDs.

Frequency (Hz)	Periodicity (Period)	Suspected Source	Coherence	PSD in B1	PSD in CB	PSD Ratio (Test/Reference)
19.3	Continuous	Computer Fans	0.22	$6.99 * 10^{-9}$	$1.69 * 10^{-10}$	42
48.4	Continuous	Computer Fans and Air Conditioners	0.63	$2.89 * 10^{-9}$	$2.39 * 10^{-10}$	¿12

TABLE IV: Noise lines found in coherence between B1 and CB. Note: As frequencies around 48Hz can come from a number of sources, we quote the ratio as an upper limit.

Frequency (Hz)	Periodicity (Period)	Suspected Source	Coherence	PSD outside B1	PSD in MC	PSD Ratio (Test/Reference)
5.3	Continuous (Daytime) Periodic (Nighttime)	SR Chiller	0.20	$5.66 * 10^{-9}$	$4.46 * 10^{-9}$	1.3
9.0	Continuous (Daytime)	B1 Chiller	0.20	$3.86 * 10^{-9}$	$1.89 * 10^{-9}$	2.0
9.4	Continuous (Daytime)	B1 Chiller	0.26	$3.07 * 10^{-9}$	$1.51 * 10^{-9}$	2.0
15.6	Continuous	Unknown	0.41	$2.51 * 10^{-9}$	$5.69 * 10^{-10}$	4.4
21.8	Continuous	Unknown	0.43	$1.08 * 10^{-9}$	$5.07 * 10^{-10}$	2.1
48.9	Continuous (Daytime)	B1 Chiller	0.41	$3.60 * 10^{-10}$	$1.55 * 10^{-10}$	2.3
58.7	Continuous (Daytime) Periodic (Nighttime)	SR Chiller	Negligible	$3.04 * 10^{-10}$	$4.53 * 10^{-10}$	0.21
87.3	Continuous (Daytime)	B1 Chiller	Negligible	$8.52 * 10^{-10}$	$3.30 * 10^{-10}$	2.6

TABLE V: Noise lines found in coherence between seismometers outside of B1 and the MC. Note: For 48.9Hz, these values were calculated during a time that the MC's cold water chiller was seen to be off, for otherwise that source dominated this line.

Frequency (Hz)	Periodicity (Period)	Suspected Source	Coherence	PSD outside MC	PSD in MC	PSD Ratio (Test/Reference)
24.2	Continuous	MC Chiller	0.22	$2.45 * 10^{-9}$	$1.20 * 10^{-9}$	2.0
38.8	Continuous	MC Chiller	0.14	$2.83 * 10^{-9}$	$1.58 * 10^{-9}$	1.7
48.9, 97.8	Periodic (21.5 Minutes)	MC Chiller	0.21	$1.09 * 10^{-7}$	$5.10 * 10^{-10}$	220

TABLE VI: Noise lines found in coherence between seismometers outside of the MC and in the MC.

Frequency (Hz)	Periodicity (Period)	Suspected Source	Coherence	PSD near WEB	PSD in WEB	PSD Ratio (Test/Reference)
7.05	Continuous	Unknown	0.38	$3.23 * 10^{-9}$	$2.50 * 10^{-9}$	1.3
24.7	Continuous	Water Pump	0.25	$1.44 * 10^{-9}$	$9.06 * 10^{-10}$	1.6
47.1	Continuous	Water Pump	0.32	$1.82 * 10^{-9}$	$1.67 * 10^{-9}$	1.1
48.8	Continuous	Water Pump	0.41	$2.50 * 10^{-9}$	$4.13 * 10^{-10}$	6.1
53.1	Continuous	HVAC	0.48	$8.97 * 10^{-10}$	$7.80 * 10^{-10}$	1.1
60.1	Continuous	HVAC	0.34	$7.82 * 10^{-10}$	$3.86 * 10^{-10}$	2.0
70.9	Continuous	Unknown	0.34	$1.95 * 10^{-9}$	$3.33 * 10^{-10}$	5.9
77.8	Continuous	Unknown	0.40	$2.20 * 10^{-9}$	$4.37 * 10^{-10}$	5.0

TABLE VII: Noise lines found in coherence between the WEB machinery and the WEB test mass. The HVAC lines were identified during a switch-off test after VSR2.

APPENDIX B: COHERENCE TABLES

Frequency (Hz)	Periodicity (Period)	Suspected Source	Coherence	PSD near NEB	PSD in NEB	PSD Ratio (Test/Reference)
13.7	Continuous	Unknown	0.36	$2.20 * 10^{-9}$	$1.07 * 10^{-9}$	2.1
20.9	Continuous	HVAC	0.46	$2.73 * 10^{-9}$	$2.23 * 10^{-9}$	1.2
22.8	Continuous	Water Pump	0.32	$2.11 * 10^{-9}$	$4.99 * 10^{-10}$	4.2
23.7	Continuous	HVAC	0.52	$7.53 * 10^{-9}$	$1.78 * 10^{-9}$	4.2
48.7,97.4	Continuous	Water Pump	0.36	$3.96 * 10^{-9}$	$1.54 * 10^{-9}$	2.6
56.9	Continuous	HVAC	0.47	$1.03 * 10^{-8}$	$6.02 * 10^{-10}$	17

TABLE VIII: Noise lines found in coherence between the NEB machinery and the NEB test mass. The HVAC lines were identified during a switch-off test after VSR2.

APPENDIX C: PSD PLOTS

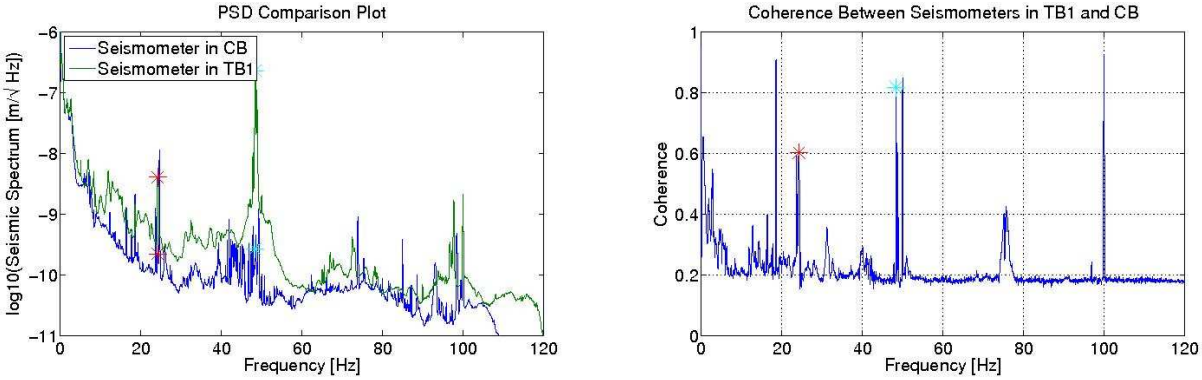

FIG. 22: Left: PSDs of the seismometers in TB1 and the CB. The peaks topped by red stars correspond to the 24.2Hz periodic line while the blue stars correspond to the 48Hz continuous line. Right: Coherence between seismometers in TB1 and the CB. The peak topped by the red star corresponds to the 24.2Hz periodic line while the blue star corresponds to the 47.9Hz continuous line.

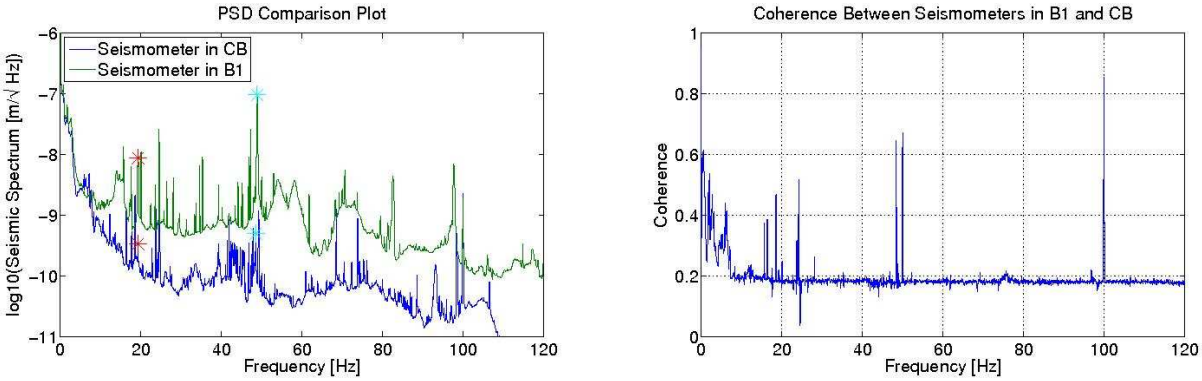

FIG. 23: Left: PSDs of the seismometers in B1 and the CB. The red stars on the left correspond to the 19.3Hz line while the blue stars on the right correspond to the 48.4Hz line. Right: Coherence between seismometers in B1 and the CB.

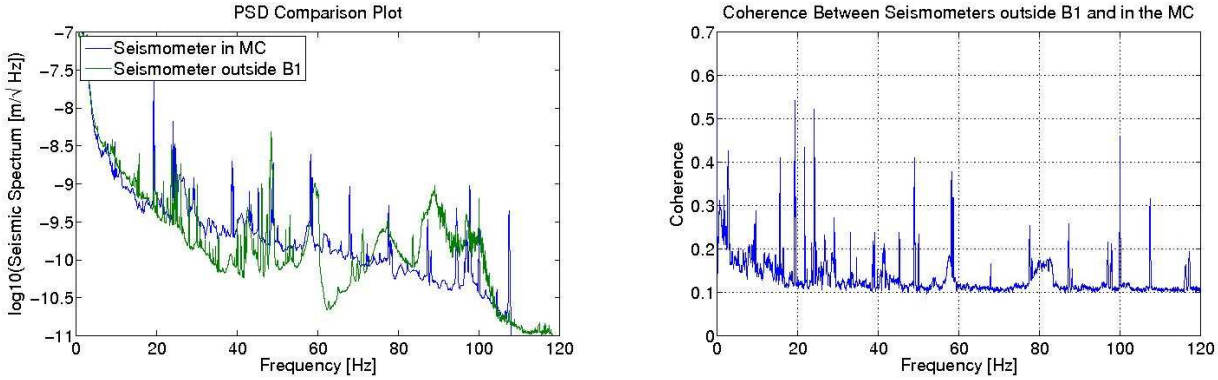

FIG. 24: Left: PSDs of the seismometers outside B1 and in the MC. Right: Coherence between seismometers outside B1 and in the MC.

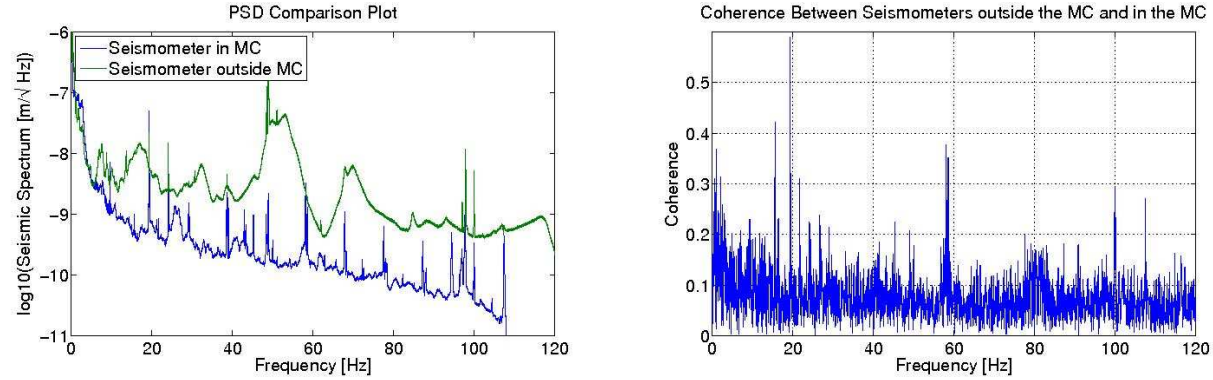

FIG. 25: Left: PSDs of the seismometers outside the MC and in the MC. Right: Coherence between seismometers outside the MC and in the MC. This plot was computed with a 60 second offset and it seems that the test probe's proximity to the chiller has made an accurate coherence estimate difficult.

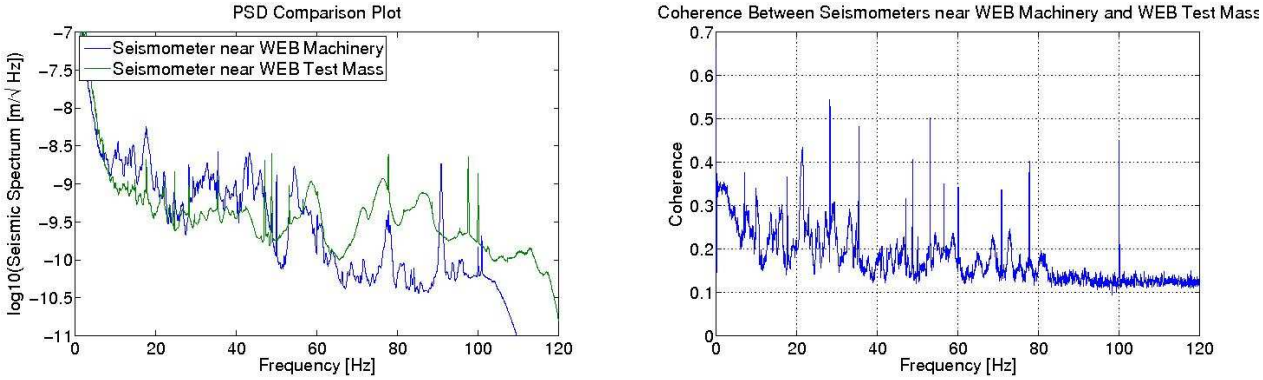

FIG. 26: Left: PSDs of the seismometers near the WEB machinery and near the WEB test mass. Right: Coherence between the seismometers near the WEB machinery and near the WEB test mass.

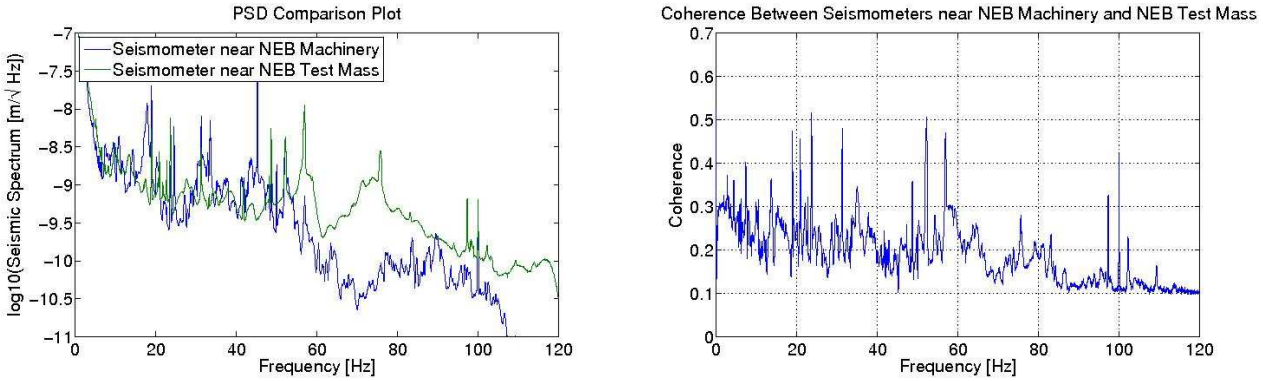

FIG. 27: Left: PSDs for the seismometers near the NEB machinery and near the NEB test mass. Right: Coherence between the seismometers near the NEB machinery and near the NEB test mass.